Electrical conductivity of fractured media: A computational study of the self-consistent method

Pål Næverlid Sævik*, Inga Berre, Morten Jakobsen and Martha Lien, University of Bergen

SUMMARY

Effective medium theory can be used to link conductivity estimation methods with prior knowledge about the distribution of fractures in the investigated geological structure. In the literature, little work has been presented on assessing the accuracy of effective medium approximations for dense networks of finite-sized fractures. We present here a systematic computational study, comparing the conductivity predictions of the popular self-consistent method with results from numerical finite-element simulations. Our results show that the self-consistent method is accurate within acceptable error bounds for a range of parameter values, in some cases even beyond the percolation limit. We also compare the percolation thresholds predicted by self-consistent theory with the thresholds obtained by a numerical percolation algorithm. For the cases we have studied, the percolation thresholds agree to a remarkable degree.

INTRODUCTION

In this work, we are concerned with the effective conductivity of statistically homogenous rocks containing small fractures. Depending on the contents of the fractures, their presence may strongly increase or decrease the observed conductivity, sometimes causing large anisotropy effects.

The presence of microfracture networks can often be inferred from the rock type and surrounding geological structures. For instance, small fractures with specific primary orientations are expected to be present in the vicinity of faults and folds (Singhal and Gupta, 1999). When using electromagnetic measurements to obtain the effective conductivity of a fractured rock, one should take care not to violate this prior knowledge. Similar arguments have also been made in the field of acoustic seismic (see, for instance, Ali and Jakobsen (2011) and the references therein).

Microfracture networks are described by the fractures' mean aperture, orientation, size, shape and spacing. To obtain a link between fracture parameters and conductivity, we can use effective medium approximations. Torquato (2002) lists different effective medium methods, e.g., the Maxwell approximation, the self-consistent scheme and the differential effective medium method. In this work, we focus on the self-consistent method, which is the only among the cited methods that exhibits percolation thresholds. Thus, it is the only candidate for use on dense networks of microfractures.

The self-consistent method is known to be first order accurate with respect to the fracture density times the conductivity contrast between fractures and matrix (Torquato, 2002). For large conductivity contrasts and dense fracture networks, there exists no analytical error estimate. To obtain a range of validity

for these conditions, one must compare the theoretical predictions with numerical upscaling for a chosen set of models.

Some numerical tests of the self-consistent method have been presented for analogous physical properties, such as fluid permeability (Pozdniakov and Tsang, 2004) and thermal conductivity (Tawerghi and Yi, 2009), with promising results. These works concern spherical/near-spherical inclusions, or isotropic/transversely isotropic media. To our knowledge, an evaluation of the self-consistent method for fully anisotropic fractured media has not been performed. For this type of geometry, we establish a novel set of simplified formulas for the self-consistent effective conductivity, with good numerical convergence properties. The analytically predicted conductivity is compared with an extensive number of estimates based on numerical simulations, both below and beyond the percolation threshold. Special attention is given to the anisotropy of the conductivity tensor, where we allow for different conductivity values in all primary spatial directions. Finally, we evaluate the percolation thresholds of the self-consistent method for a sample of chosen fracture geometries, using an accurate numerical percolation algorithm.

THEORY

To link fracture parameters with effective conductivity, a model for fracture shape and distribution is required. As is commonly done in effective medium theory, we assume here that the fractures are shaped as very thin oblate spheroids, distributed randomly in space. Furthermore, we assume that the fractures can be divided into a finite number of families, according to their orientations, apertures and conductivities. We refer to each fracture family, as well as the background matrix, as separate solid phases.

Following Willis (1977), we have from the definition of the effective conductivity $\bar{\sigma}$ and the average electrical field $\bar{\mathbf{E}}$, that

$$\bar{\sigma}\bar{\mathbf{E}} = \sigma_0\bar{\mathbf{E}} + \sum_{i=1}^{N} \phi_i (\sigma_i - \sigma_0) \mathbf{E}_i, \qquad (1)$$

where ϕ_i, σ_i and $\mathbf{E}_i$ are the volume fraction, conductivity and average field of phase i, respectively. By convention, we will denote the matrix phase by the subscript 0. As a first step, we assume that the interactions between individual fractures can be neglected. In this case, $\bar{\mathbf{E}}$ and $\mathbf{E}_i$ are related by the following relation (Torquato, 2002),

$$\mathbf{E}_i = (\mathbf{I} + \mathbf{A}_i (\sigma_0) (\sigma_i - \sigma_0))^{-1} \bar{\mathbf{E}}. \qquad (2)$$

The depolarization tensor $\mathbf{A}_i$ depends on the background medium, as well as the shape and orientation of the fractures, and can be calculated from the current conservation equation for the single-inclusion problem. We will return to this later.

Equation (2) is strictly valid only when the background medium has a homogenous conductivity σ_0. Since each fracture is surrounded by a heterogenous material of effective conductivity $\bar{\sigma}$, we can obtain a better approximation by substituting σ_0 with $\bar{\sigma}$ in (2). Combining with (1), we arrive at the self-consistent approximation,

$$\bar{\sigma} = \sigma_0 + \sum_{i=1}^{N} \phi_i \left(\sigma_i - \sigma_0\right) \left(\mathbf{I} + \mathbf{A}_i\left(\bar{\sigma}\right) \left(\sigma_i - \bar{\sigma}\right)\right)^{-1}. \quad (3)$$

The formula is an implicit relationship for $\bar{\sigma}$ that must be solved numerically, i.e., by a fixed-point iteration. For resistive inclusions, a straightforward fixed-point iteration based on (3) will diverge. In this case, we can reformulate (3) in terms of *inverse* conductivities to obtain a scheme with better convergence properties.

Equation (3) is sometimes called the *asymmetric* self-consistent approximation, since it gives special treatment to the matrix material. An alternative approach, not considered in this paper, is to treat matrix and inclusions in a symmetric fashion, as in Barthélémy (2009). In the symmetric self-consistent method, both the matrix and the fractures are treated as a collection of ellipsoidal inclusions. Traditionally, this approach has mostly been recommended for media that possess phase symmetry, such as polycrystals (Willis, 1977; Torquato, 2002).

For isotropic media and spheroidal inclusions, formulas for the depolarization tensor $\mathbf{A}_i$ can be found in many sources, e.g., Eshelby (1957) or Landau and Lifshitz (1960). For anisotropic media, the expression for $\mathbf{A}_i$ becomes more complicated. We state here the main result, and refer to Barthélémy (2009) for a full derivation. To avoid cluttering the formulas, we ignore the fracture family subscript i in the remainder of the section.

Suppose that the unit vector $\mathbf{n}$ defines the orientation of an oblate spheroidal inclusion of aspect ratio $\varepsilon < 1$, embedded in a matrix of anisotropic conductivity $\bar{\sigma}$. Let $\mathbf{H} = \mathbf{I} - \left(1 - \varepsilon^2\right) \mathbf{nn}$, where $\mathbf{nn}$ is an outer product, and let $\bar{\sigma}^{1/2}$ denote the positive definite square root of $\bar{\sigma}$. Let $\mathbf{QKQ}^{\top}$ be an eigenvalue decomposition of the matrix $\gamma \bar{\sigma}^{-1/2} \mathbf{H} \bar{\sigma}^{-1/2}$, where we have added the normalization constant $\gamma = \sqrt[3]{\det \bar{\sigma}}$ for later convenience. Then the depolarization tensor $\mathbf{A}$ is given by

$$\mathbf{A} = \bar{\sigma}^{-1/2} \mathbf{Q} \mathbf{D}\left(\mathbf{K}\right) \mathbf{Q}^{\top} \bar{\sigma}^{-1/2},$$

where the diagonal matrix $\mathbf{D}$ is a nonlinear function of $\mathbf{K}$, defined by Barthelemy in terms of Legendre elliptic integrals. For our purposes, it is more convenient to use the Carlson elliptic integrals, for which efficient numerical evaluation methods are available (Carlson, 1995). $\mathbf{D}$ is then given by

$$r_1 = \frac{1}{2} \int_0^{\infty} \frac{dt}{\left(t + k_1\right) \sqrt{\left(t + k_1\right)\left(t + k_2\right)\left(t + k_3\right)}},$$

$$r_2 = \frac{1}{2} \int_0^{\infty} \frac{dt}{\left(t + k_2\right) \sqrt{\left(t + k_1\right)\left(t + k_2\right)\left(t + k_3\right)}},$$

$$d_1 = \varepsilon r_1, d_2 = \varepsilon r_2, d_3 = 1 - d_1 - d_2,$$

where k_1, k_2, k_3 and d_1, d_2, d_3 are the diagonal elements of $\mathbf{K}$ and $\mathbf{D}$, respectively. For convenience, we have assumed that $k_1 \geq k_2 \geq k_3$, which in turn implies $d_1 \leq d_2 \leq d_3$.
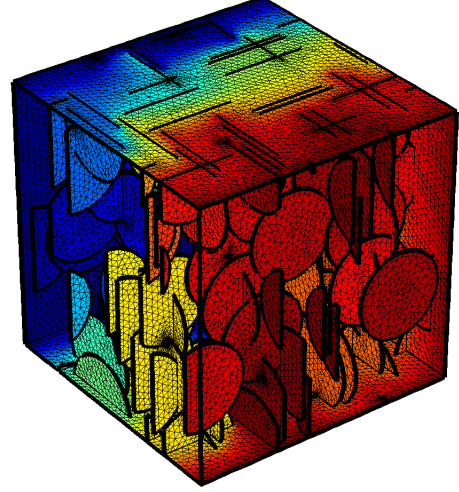

Figure 1: Distribution of electrical potential in two synthetic conductive fracture sets. Total fracture density is 0.4.

Simplified expressions in the flat oblate limit

We will now develop a novel set of simplified formulas for the effective conductivity when $\varepsilon \ll 1$, which corresponds to very flat oblate spheroids. For simplicity, we assume that the conductivity within the fractures is isotropic. First, let us define the following symbols:

$$\mathbf{B}^{\mathrm{I}} = \varepsilon \mathbf{A}^{-1}, \qquad \mathbf{B}^{\mathrm{III}} = \varepsilon \left(\mathbf{I} - \mathbf{A}\bar{\sigma}\right)^{-1} \bar{\sigma}^{-1},$$

$$\mathbf{B}^{\mathrm{II}} = \varepsilon \mathbf{A}^{-1} - \varepsilon \bar{\sigma}, \qquad \mathbf{B}^{\mathrm{IV}} = \varepsilon \left(\mathbf{I} - \mathbf{A}\bar{\sigma}\right)^{-1} \mathbf{A},$$

$$\omega = 1/\sigma\varepsilon, \qquad \eta = \sigma/\varepsilon,$$

$$\rho = Nr^3 = \frac{3\phi}{4\pi\varepsilon},$$

where N is the number of fractures per volume, and r is the fracture radius. We begin our derivation with Equation (2), which is equivalent to any of the following two expressions,

$$\mathbf{E} = \omega \left(\omega \mathbf{B}^{\mathrm{II}} + \mathbf{I}\right)^{-1} \mathbf{B}^{\mathrm{I}} \bar{\mathbf{E}}, \quad (4)$$

$$\varepsilon \mathbf{E} = \left(\eta \mathbf{B}^{\mathrm{IV}} + \mathbf{I}\right)^{-1} \mathbf{B}^{\mathrm{III}} \bar{\sigma} \bar{\mathbf{E}}. \quad (5)$$

Combining (2), (3) and (4), assuming $\sigma_0 \ll \sigma_i$, we have the following expression for the effective conductivity:

$$\bar{\sigma} = \sigma_0 + \frac{4}{3}\pi \sum_{i=1}^{N} \rho_i \left(\omega_i \mathbf{B}_i^{\mathrm{II}} + \mathbf{I}\right)^{-1} \mathbf{B}_i^{\mathrm{I}}. \quad (6)$$

For $\varepsilon \ll 1$, the $\mathbf{B}$ tensors are asymptotically equivalent to

$$\mathbf{B}^{\mathrm{I}} = \mathbf{B}^{\mathrm{II}} = \bar{\sigma}^{1/2} \mathbf{Q} \begin{bmatrix} 1/r_1 & & \\ & 1/r_2 & \\ & & 0 \end{bmatrix} \mathbf{Q}^{\top} \bar{\sigma}^{1/2},$$

where r_1 and r_2 are defined as above.

Similarly, combining (2), (3) and (5), assuming $\sigma_0 \gg \sigma_i$, we can express the inverse of the effective conductivity as

$$\bar{\sigma}^{-1} = \sigma_0^{-1} + \frac{4}{3}\pi \sum_{i=1}^{N} \rho_i \left(\eta_i \mathbf{B}_i^{\mathrm{IV}} + \mathbf{I}\right)^{-1} \mathbf{B}_i^{\mathrm{III}}. \quad (7)$$
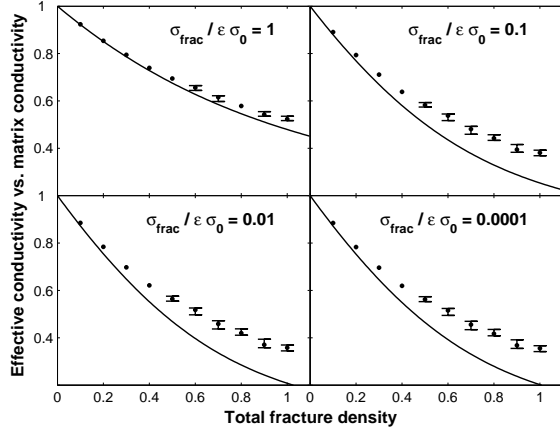
Figure 2: Transversal effective conductivity for two orthogonal resistive fracture sets. The solid line is the self-consistent method, the dots are sample medians from numerical simulations, and the bars show the interquartile range.

For $\varepsilon \ll 1$, we have the asymptotic equivalence

$$\mathbf{B}^{\mathrm{III}} = \mathbf{B}^{\mathrm{IV}} = \bar{\sigma}^{-1/2}\mathbf{Q} \begin{bmatrix} 0 & & \\ & 0 & \\ & & 1/(r_1 + r_2) \end{bmatrix} \mathbf{Q}^{\top} \bar{\sigma}^{-1/2}.$$

Both (6) and (7) can be efficiently evaluated using a simple fixed-point iteration scheme.

NUMERICAL EXAMPLES

We computed the effective conductivity for a range of different fracture parameters (fracture density, aperture and conductivity), and compared the results with predictions from self-consistent theory. For each set of parameters, we generated random distributions of 100 oriented discs (flat cylinders) of equal size inside a unit cube. Figure 1 shows a sample configuration. We applied unit potential differences on two opposing sides, and no-flux conditions on the remaining sides. Finally, we used a commercial finite-element software to compute the flux through the cube, from which the effective conductivity was found. The aperture of the discs was chosen to be the average thickness of the corresponding oblate spheroid in the self-consistent model. Preliminary numerical tests suggest that the simplification of substituting spheroids with discs has little impact on the computed effective conductivity for small aspect ratios (i.e., $\varepsilon \leq 0.01$).

Numerical errors

In numerical tests like this, there are three primary error sources that may impact the calculated effective conductivity:

- Finite-size effects
- Statistical variation
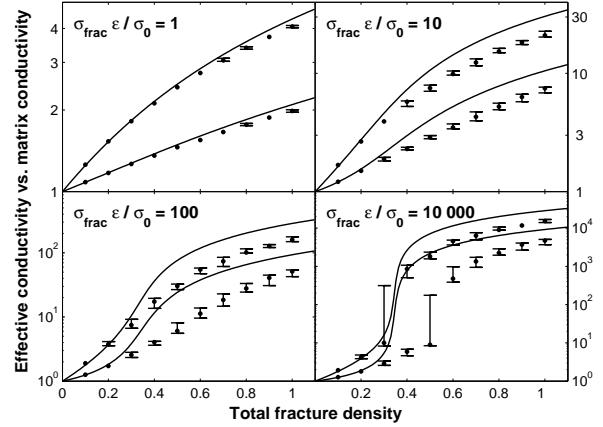- Discretization errors

Figure 3: Effective conductivity, in the directions of smallest and largest conductivity, for two orthogonal conductive fracture sets. The solid line is the self-consistent method, the dots are sample medians from numerical simulations, and the bars show the interquartile range.

The effects of running the simulation on a finite volume are two-fold. First of all, the electrical field may be locally disturbed near the boundaries. Secondly, the computations may not be able to correctly capture the effects of fracture clusters that are larger than the computational domain. This is especially true near the percolation threshold. To assess the significance of these errors, we ran a series of comparison tests, using sample sizes as low as 20 discs per unit volume. In addition, we solved for a sample of the geometries using periodic boundary conditions. The tests showed that a larger fracture density was required in order to obtain percolation if the sample size was small. Other than this, the results proved to be robust to reductions in the sample size. Neither did the switching to periodic boundary conditions affect the results significantly.

The second main error source is the uncertainty caused by statistical variation. For each set of parameter values, we used at least 10 different realizations of the fracture geometry, and computed the median of the effective conductivities obtained. A different sample of realizations would have given another conductivity estimate, thus the result is stochastic variable. The variability is typically low for fracture densities below the percolation threshold, intermediate above the threshold, and large around the threshold itself. In our presentation of the results, we have chosen to visualize this by plotting the sample interquartile range.

The numerical discretization error is the third main error source. To assure that such errors did not contribute significantly to the results, we performed a series of tests with varying grid size and element order. For some of the tests, we also used the adaptive meshing feature provided by the software. The final results were computed using linear elements and a fine unstructured grid, with 100.000-150.000 degrees of freedom. For these meshing parameters, we found that the numerical errors were smaller than the statistical uncertainty.

Results

The first class of fracture geometry we considered, is the case of two orthogonally oriented fracture sets of equal fracture density, conductivity and aperture, embedded in a matrix of isotropic conductivity. Thus we have $\rho_1 = \rho_2$, $\sigma_1 = \sigma_2 = \sigma_{frac}$ and $\varepsilon_1 = \varepsilon_2 = \varepsilon$, and the effective conductivity is transversely isotropic. Since we are considering flat inclusions, both the numerical and the analytical results depend on the conductivity and aperture through the ratio $\sigma_{frac}/\varepsilon$ for resistive fractures and $\sigma_{frac}\varepsilon$ for conductive fractures. For instance, $\sigma_{frac}/\varepsilon\sigma_0 = 1$ may indicate a conductivity contrast of 100 and an aspect ratio of 0.01. In the numerical simulations, we calculated the effective conductivity for different values of $\sigma_{frac}/\varepsilon$ and $\sigma_{frac}\varepsilon$, as well as the total fracture density $\rho_T = \rho_1 + \rho_2$.

In Figure 2, we have shown the results for resistive fractures in the transverse direction, along with the analytical predictions from Equation (7). As expected, the agreement is good for small fracture densities and conductivity contrasts. When the fracture network is globally disconnected ($\rho < 0.3$), or when $\sigma_{frac}/\varepsilon\sigma_0 \leq 1$, the discrepancy between the analytical and numerical result is less than 10%. For higher fracture densities and conductivity contrasts, the self-consistent method underpredicts the conductivity by a significant amount. At $\rho_T = 1$, the numerical results are up to 75% larger than the analytically predicted values.

Secondly, we considered two orthogonal conductive fracture sets where the fracture density of one set was twice as large as the other. This causes anisotropy both in the transverse and vertical direction. The effective conductivity is largest in the vertical direction, which is parallel to both fracture sets. The smallest conductivity is seen in the direction orthogonal to the set of largest fracture density. Numerical results and analytical predictions (using Equation (6)) for these two directions are shown in Figure 3. The results for the third orthogonal direction are qualitatively similar.

Again, we see that the predictions by the self-consistent method are good in the case of smaller conductivity contrasts. For larger contrasts, the method overpredicts the conductivity by up to 75% once again, compared to the numerical estimates. It should be noted that the numerical results near the percolation threshold are uncertain, both because of the statistical uncertainty (visualized in the figure), and because finite-size effects cause the percolation threshold to appear at a different location. Although the method seems to overpredict conductivity, the coefficient of anisotropy is still correctly estimated for $\sigma_{frac}\varepsilon/\sigma_{mat} \leq 10$. For larger values of the aperture-conductivity product, the anisotropy is difficult to estimate accurately from the numerical results.

To assess the validity of the percolation thresholds predicted from self-consistent theory, we used the accurate and efficient percolation algorithm proposed by Yi and Tawerghi (2009). We considered two sets of fractures, and varied the proportional amounts of the sets, as well as their orientations. The size of all fractures was taken to be equal.

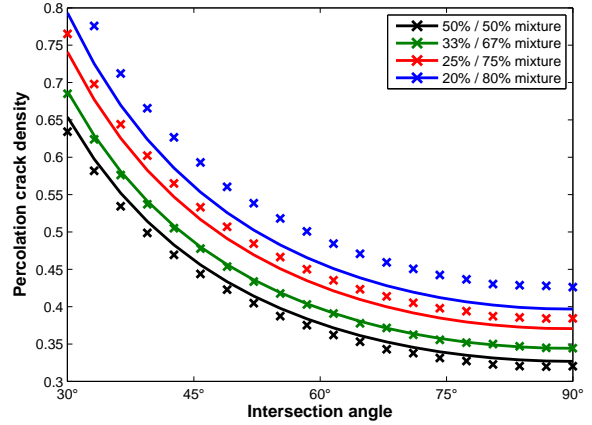The results are reported in Figure 4. We find that the predicted

Figure 4: Percolation thresholds of two fracture sets, with varying mixture ratios and intersection angles. The solid lines represent the self-consistent estimates for the critical fracture density, and crosses represent the numerically computed values.

thresholds agree with the numerical results to a remarkable degree. Both are inversely proportional to the sine of the angle between the fractures, and both depend on the fracture proportions to about the same degree. Although the results look promising, Torquato (2002) suggests from theoretical considerations that the percolation thresholds obtained from self-consistent approximations should be treated with caution. Further work is required in order to determine if the accordance shown in Figure 4 is to be expected for more than two fracture sets.

CONCLUSIONS

We have proposed a new set of formulas for calculating the self-consistent effective conductivity of fractured media. Through carefully designed numerical experiments, we have shown that the method is capable of estimating the anisotropic effective conductivity both below and above the percolation threshold. The quality of the estimates are good for lower fracture densities and intermediate fracture-matrix conductivity contrasts. For higher fracture densities, the discrepancy is larger, but may still be useful as a rough estimate. Using a numerical percolation algorithm, we have also demonstrated that the percolation thresholds obtained from the self-consistent method are remarkably accurate when applied to two sets of fractures with different orientations.

ACKNOWLEDGEMENTS

REFERENCES

Ali, A., and M. Jakobsen, 2011, Seismic characterization of reservoirs with multiple fracture sets using velocity and attenuation anisotropy data: Journal of Applied Geophysics, **75**, 590–602.

Barthélémy, J. F., 2009, Effective permeability of media with a dense network of long and micro fractures: Transport in Porous Media, **76**, no. 1, 153–178.

Carlson, B. C., 1995, Numerical computation of real or complex elliptic integrals: Numerical Algorithms, **10**, 13–26.

Eshelby, J. D., 1957, The determination of the elastic field of an ellipsoidal inclusion, and related problems: Proceedings of the Royal Society of London. Series A. Mathematical and Physical Sciences, **241**, 376–396.

Landau, L. D., and E. M. Lifshitz, 1960, Electrodynamics of continuous media: Pergamon Press.

Pozdniakov, S., and C. F. Tsang, 2004, A self-consistent approach for calculating the effective hydraulic conductivity of a binary, heterogeneous medium: Water resources research, **40**, W05105.

Singhal, B. B. S., and R. P. Gupta, 1999, Applied hydrogeology of fractured rocks: Kluwer Academic Publishers.

Tawerghi, E., and Y. B. Yi, 2009, A computational study on the effective properties of heterogeneous random media containing particulate inclusions: Journal of Physics D: Applied Physics, **42**, 175409.

Torquato, S., 2002, Random heterogenous materials: Springer-Verlag.

Willis, J. R., 1977, Bounds and self-consistent estimates for the overall properties of anisotropic composites: Journal of the Mechanics and Physics of Solids, **25**, 185–202.

Yi, Y. B., and E. Tawerghi, 2009, Geometric percolation thresholds of interpenetrating plates in three-dimensional space: Physical Review E, **79**, 041134.